Artifacts in Kirchhoff common image gathers

Christiaan C. Stolk and William W. Symes, Rice University*

Summary

Strongly refracting velocity structure produces image artifacts in prestack Kirchhoff depth migration, i.e. coherent reflectivity not corresponding to actual reflectors. This effect occurs when the velocity is exactly correct, for any binning scheme (common source, common offset, common angle). In particular, image gathers produced by prestack Kirchhoff migration are not flat even when the velocity is correct. This result casts doubt on the prospects for Kirchhoff based migration velocity analysis in regions of strong lateral heterogeneity.

Introduction

Strong refraction ("complex structure") is understood to constitute an impediment to seismic imaging and velocity analysis based on Kirchhoff migration. Nolan demonstrated that image gathers (common source, common offset,...) and partial images from individual data bins are generally riddled with *image artifacts*, i.e. coherent reflectivity not corresponding to actual reflectors, in strongly refracting media, even when the velocity model used is correct and all arrivals are used in the migration process (Nolan and Symes, 1996; Nolan and Symes, 1997). Ray theory determines the positions of artifacts (and correct image components), and these are stable under velocity perturbations. When the velocity is correct, the artifacts move out with bin parameter, whereas the correct image components do not: this accounts for the disappearance of the artifacts in the final stacked image, as per (Ten Kroode et al., 1998). However image artifacts are present with strength equal to (or even sometimes greater than) that of correct image components in the prestack image volume. In effect, *image gathers are generally not flat, even when the correct velocity is used.* Flattening image gathers is the basis of effective velocity analysis, either directly or indirectly (through velocity spectrum peak location) (Yilmaz, 1987; Taner and Koehler, 1969). Thus Nolan's result casts doubt on the possibility of velocity analysis using Kirchhoff migration of any sort in complex velocity structures, at least with common source binning.

Common scattering angle prestack depth migration, an extension of the p-τ imaging concept to laterally heterogeneous media, has been studied recently by a number of authors in both Kirchhoff (Xu et al., 2001; Brandsberg-Dahl et al., 1999)), and wave equation (Prucha et al., 1999; Sava et al., 2001) variants. Perusal of the examples presented in these papers suggests that angle images and angle domain image gathers appear to be quite a bit "cleaner" than their offset domain analogues. In fact, (Xu et al., 2001) assert that common angle prestack Kirchhoff depth migration does not produce image artifacts. If true, this observation would single out the common angle domain as particularly appropriate for velocity analysis. The examples presented in (Xu et al., 2001), however, are too complex to convincingly support such a conclusion, nor could a few examples in themselves establish such a categorical assertion.

This abstract presents a common framework for understanding the presence or absence of image artifacts in both offset and angle domain Kirchhoff migration. In another place (Stolk, 2001) we have presented a mathematical analysis of this question which establishes the existence of kinematic artifacts (i.e. in map migration, using the ray geometry associated with Kirchhoff migration) for strongly refracting velocity models. In this paper we use an example very similar to that of (Nolan and Symes, 1996) to show that image artifacts may be present in prestack Kirchhoff images, in *both* the common angle and common offset domains. In particular, contrary to the assertion in (Xu et al., 2001), angle domain image gathers are not in general flat even when the velocity is correct. At least from the point of view of Kirchhoff migration, the angle domain does not appear to be categorically superior to the offset domain for velocity analysis.

The next section presents a mathematical description of Kirchhoff depth migration, originally developed in (Stolk and De Hoop, 2002), sufficiently general to encompass both common offset and common angle imaging. Note that this formulation includes all arrivals in image formation: the necessity of including all arrivals is implicit in the results of (Ten Kroode et al., 1998), and was explicitly demonstrated in (Operto et al., 2001). In the following section we use an implementation of this operator to examine angle and offset domain image volumes for a strongly refracting 2D Gaussian lens. We end the paper with a discussion of the implications for velocity analysis, the generic nature of these results, and the relation with recent work on wave equation angle domain imaging.

Prestack Kirchhoff imaging formulas, theory

A reflecting pair of geometrical optics rays can be parametrized by the reflection point x in the subsurface, and the take off angles for the source and receiver rays (β, α). The intersection point $\mathbf{s}(x, \beta)$ of the source ray with the acquistion plane can be determined together with the corresponding travel time $\mathbf{t}_{\rm s}(x, \beta)$, and similarly for the receiver $\mathbf{r}(x, \alpha), \mathbf{t}_{\rm r}(x, \alpha)$, see Figure 1.

Inversion of the map (x, β) to (x, s) yields the angle function $\alpha^{(i)}(x, s)$, and the one-way travel time function $T_1^{(i)}(x, s)$. These functions are multivalued: index the

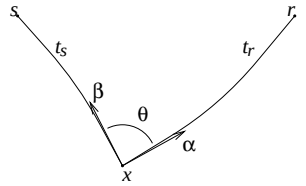

Fig. 1: Reflected ray pair, notation

branches by i. Each branch is defined on a domain $D^{(i)}$ of (x, s) pairs, which generally varies from branch to branch. The two way travel time $T^{(i,j)}(x, s, r)$ is defined by

$$T^{(i,j)}(x, s, r) = T_1^{(i)}(x, s) + T_1^{(j)}(x, r). \tag{1}$$

In two dimensions we can define the opening angle $\theta^{(i,j)}(x, s, r)$ by

$$\theta^{(i,j)}(x, s, r) = \alpha^{(j)}(x, r) - \alpha^{(i)}(x, s). \tag{2}$$

(for three dimension see (Burridge and Beylkin, 1988)). The domains $D^{(i,j)}$ of these functions consist of the points (x, s, r) with $(x, s) \in D^{(i)}$ and $(x, r) \in D^{(i)}$. We also define a cutoff (mute) function $A^{(i,j)}(x, s, r)$, that is equal to one on a subset of of $D^{(i,j)}$ and goes to zero smoothly near the boundary. The cutoff can be calculated as a product of cutoffs for the source and receiver domains.

A Kirchhoff imaging formula is given by

$$f(x) = \sum_{i,j} \int \mathrm{d}s\, \mathrm{d}r\, A^{(i,j)}(x, r, s) \times (H^{n-1-\sigma^{(i)}-\sigma^{(j)}} d)(r, s, T^{(i,j)}(x, r, s)). \tag{3}$$

Here H is the Hilbert transform with respect to time, and $\sigma^{(i)}$ is the KMAH index, to account for the phase shift that occurs when the rays go through a caustic. The *prestack* imaging formulas are obtained by restricting the integral over (s, r) to a constant value of the image parameter. The latter can be viewed as a function $\mathbf{e}$ of (x, α, β), and hence as a multivalued function $\mathbf{e}^{(i,j)}(x, s, r)$, defined on $D^{(i,j)}$. Restricting the integral (3) by inserting a δ-function we obtain the following form for the prestack imaging formula

$$f_e(x) = \sum_{i,j} \int \mathrm{d}s\, \mathrm{d}r\, A^{(i,j)}(x, s, r)\delta(e - \mathbf{e}^{(i,j)}(x, s, r)) \times (H^{n-1-\sigma^{(i)}-\sigma^{(j)}} d)(s, r, T^{(i,j)}(x, s, r)), \tag{4}$$

The parameter e can be offset, angle, source position, ... For the offset case we have

$$\mathbf{e}^{(i,j)}(x, s, r) = r - s.$$

In the angle case $\mathbf{e}^{(i,j)}(x, s, r) = \theta^{(i,j)}(x, s, r)$ as defined in (2).

To discretize (4), a numerical approximation to the δ-function was chosen based on adjoint interpolation. If the center e_0 of the δ-function is between two grid points $\hat{e}_1, \hat{e}_2$, then there is contribution proportional to $|e_0 - \hat{e}_2|$ at $\hat{e}_1$, and similarly with $1, 2$ interchanged.

Example

In this section we study a simple example where the medium contains a horizontal reflector below a low velocity lens that leads to multipathing. This example is very similar to the one used in (Nolan and Symes, 1996). The lens is located at 1 km below the origin of the coordinate system. Coordinates are written (x_1, x_2); x_1 is the horizontal coordinate, x_2 the vertical coordinate. The velocity is given by

$$c(x_1, x_2) = 1 - 0.4\, e^{-9(x_1^2+(x_2-1)^2)}\mathrm{km/s}. \tag{5}$$

We assume a horizontal reflector is located at $x_2 = 2$ km. Background velocity and reflector are displayed in Figure 2, together with some of the rays and wave fronts. A triplication occurs below the lens.

A synthetic dataset was computed for this medium using a finite difference wave equation solver. The data consists of 401 shotrecords for s with interval 0.01 km from -2 to 2 km. For each shot the response was recorded at 401 receivers also with interval 0.01 km, from -2 to 2 km. No absorbing boundary conditions were applied, but the domain was chosen so large that reflections from the boundary arrived significantly later, with different moveout, so that there is no significant effect on the images. A shot record for $s = 0.5$ km is displayed in Figure 3. A stacked image, obtained by applying (3) to the data, is displayed in Figure 4. The reflector is indeed recovered at the correct position, as predicted by (Ten Kroode et al., 1998).

Imaging equations, derived in (Stolk, 2001), predict the position of coherent reflectivity in the image, from the positions of wave fronts in the data and the normals to these wave fronts. Given a point (s, r, t) in acquisition space, and slownesses $(p_\mathrm{s}, p_\mathrm{r})$, the positions (x, e) of both correct and artifact contributions can be determined. Solutions can be found numerically by rewriting the ray and imaging equations in a suitable form and applying a numerical ordinary differential equation solver and a root finding procedure that can be found in standard mathematical software (we used the software package Mathematica^{TM}). In (Stolk, 2001) we applied this procedure to the model just described. Here we compare these kinematic predictions with images produced by Kirchhoff migration of the synthetic data.

The offset case: We have computed ray pairs that lead to contributions to the image for a reflecting element at $x = (0.303, 2)$, with opening angle 28.05 degree (chosen so that the offset was equal to 1). The kinematic computation predicts that the reflected energy in the data due to this reflecting element gives rise to three image elements,

one correct and two artifacts. A constant offset image for offset $h = 1$ km, with part of the ray pairs overlaid, shows that indeed this energy is imaged at the reflection points of the different ray pairs, see Figure 5.

Using the imaging equations we predicted the positions of wave fronts in the offset CIG for horizontal position $x_1 = 0.3$ km, in effect a *map migration*. These are presented as the light gray lines in Figure 6. The graylevel plot in Figure 6 represents the Kirchhoff migrated CIG. All the events predicted from the kinematics are clearly visible.

The angle case: In the angle case we did similar calculations. An angle domain Kirchhoff migration CIG is given in Figure 7, together with the predictions obtained by solving the imaging equations. Again all the predicted kinematic artifacts can be observed in the Kirchhoff migration.

Discussion

The examples presented here and in (Nolan and Symes, 1996) establish that image artifacts, i.e. coherent reflectivity not corresponding to actual reflectors, can exist in prestack image volumes for Kirchhoff prestack depth migration in the common source, offset and angle domains, for sufficiently strongly refracting velocity models. In particular, formulation of Kirchhoff migration in the common angle domain does not suppress imaging artifacts, contrary to assertions in the literature (Xu et al., 2001).

Perhaps the most striking conclusion to be drawn from our analysis is that image gathers produced by Kirchhoff migration are not in general flat in the presence of strong refraction, even when the velocity model is precisely correct, because of the presence of prestack imaging artifacts. Since flattening image gathers is the underlying mechanism of practical velocity analysis, our examples cast doubt on the possibility of successful determination of velocity models with strong lateral heterogeneity via velocity analysis based on Kirchhoff migration.

Very recently, some evidence has emerged that *wave equation common angle migration* (Prucha et al., 1999; Sava et al., 2001) does *not* generate prestack image artifacts at correct migration velocity (Stolk and De Hoop, 2001). One could perhaps understand this effect heuristically by noting that the wave equation imaging condition is entirely local, and thus avoids the global confusion of energy paths suffered by Kirchhoff migration - see (Bevc, 1997) for discussion of a similar concept. In any case, the implications of the results in (Stolk and De Hoop, 2001) for velocity analysis remain to be explored.

Acknowledgement: This work was supported in part by the sponsors of The Rice Inversion Project.

References

Bevc, D., 1997, Imaging complex structures with semirecursive Kirchhoff migration: Geophysics, **62**, 577–588.

Brandsberg-Dahl, S., De Hoop, M., and Ursin, B., 1999, Velocity analysis in the common scattering-angle/azimuth domain: 69th Ann. Internat. Mtg., Soc. of Expl. Geophys., 1715–1718.

Burridge, R., and Beylkin, G., 1988, On double integrals over spheres: Inverse Problems, **4**, no. 1, 1–10.

Nolan, C. J., and Symes, W. W., 1996, Imaging and coherency in complex structure: 66th Ann. Internat. Mtg., Soc. of Expl. Geophys., 359–363.

Nolan, C. J., and Symes, W. W., 1997, Global solution of a linearized inverse problem for the wave equation: Comm. Partial Differential Equations, **22**, no. 5-6, 919–952.

Operto, S., Xu, S., and Lambaré, G., 2001, Can we image quantitativley complex models with rays?: Geophysics, **65**, 1223–1238.

Prucha, M., Biondi, B., and Symes, W., 1999, Angle-domain common image gathers by wave-equation migration: 69th Ann. Internat. Mtg., Soc. of Expl. Geophys., 824–827.

Sava, P., Biondi, B., and Fomel, S., 2001, Amplitude-preserved common image gathers by wave-equation migration: 71th Ann. Internat. Mtg., Soc. of Expl. Geophys., 296–299.

Stolk, C. C., and De Hoop, M. V., December 2001, Seismic inverse scattering in the 'wave-equation' approach, Preprint 2001-047, The Mathematical Sciences Research Institute, http://msri.org/publications/preprints/2001.html.

Stolk, C. C., and De Hoop, M. V., 2002, Microlocal analysis of seismic inverse scattering in anisotropic elastic media: Comm. Pure Appl. Math., **55**, no. 3, 261–301.

Stolk, C. C., 2001, Microlocal analysis of the scattering angle transform, Preprint, Dept. of Computational and Applied Mathematics, Rice University, http://www.caam.rice.edu/ cstolk/angle.ps, To appear in Comm. in Partial Differential Equations.

Taner, M., and Koehler, F., 1969, Velocity spectra: digital computer derivation and application of velocity functions: Geophysics, **34**, 859–881.

Ten Kroode, A. P. E., Smit, D. J., and Verdel, A. R., 1998, A microlocal analysis of migration: Wave Motion, **28**, 149–172.

Xu, S., Chauris, H., Lambaré, G., and Noble, M., 2001, Common angle migration: A strategy for imaging complex media: Geophysics, **66**, no. 6, 1877–1894.

Yilmaz, O., 1987, Seismic data processing: Investigations in Geophysics No. 2.

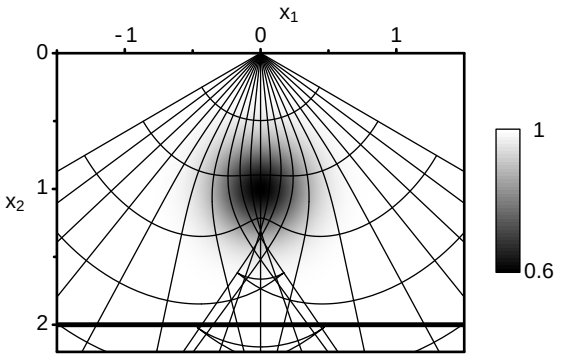

Fig. 2: Background medium, reflector and rays

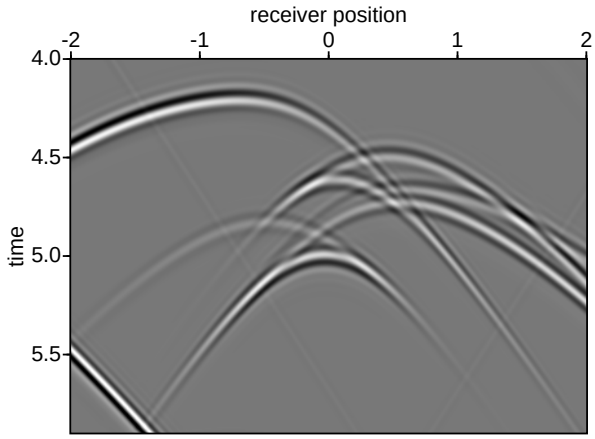

Fig. 3: Shot record at $s = -0.5$ km.

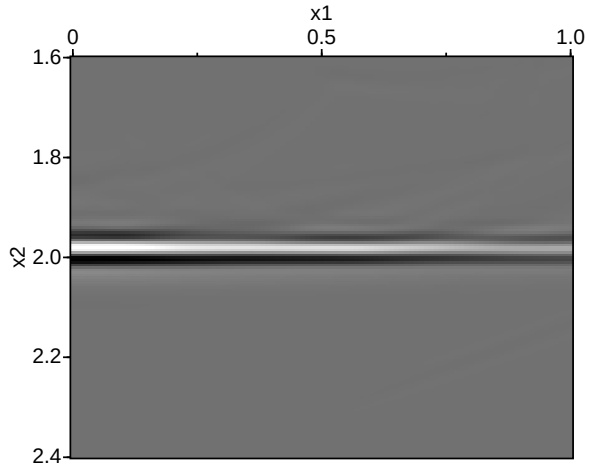

Fig. 4: Stacked image

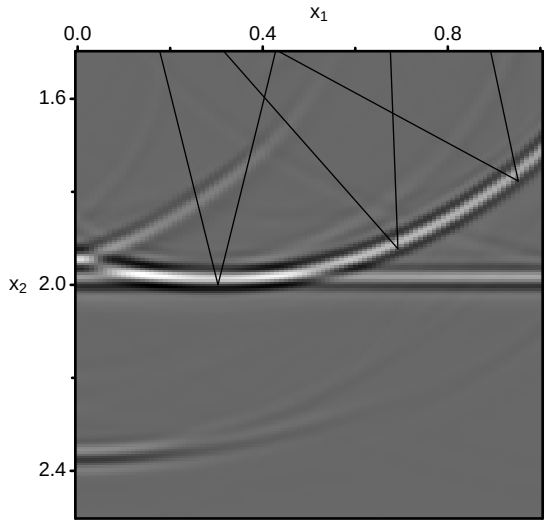

Fig. 5: Image from offset 1 km. Rays corresponding to the reflection produced by a reflecting element at $x = (0.303, 2)$ are shown. All three of these ray pairs satisfy the imaging condition. Only one of them images at the correct location. The other two contribute to artifact formation.

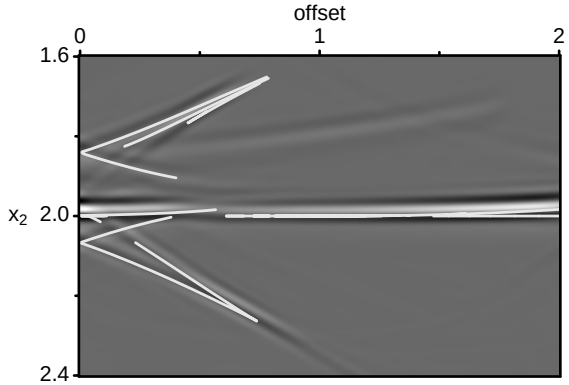

Fig. 6: Offset domain CIG, $x_1 = 0.3$ km, kinematic prediction and Kirchhoff migration.

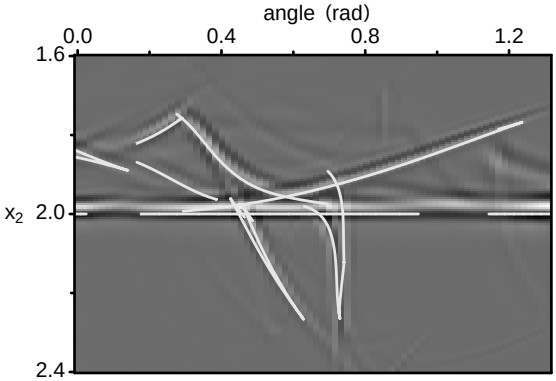

Fig. 7: Angle domain CIG, $x_1 = 0.3$ km, kinematic prediction and Kirchhoff migration.